A New Type of Carbon Nanostructure Formed Within a Metal-Matrix

[1]Lourdes Salamanca-Riba, [1]Romaine Isaacs, [2]Azzam N. Mansour, [3]Adam Hall, [2]David R. Forrest, [4]Melburne C. LeMieux, and [5]Jason Shugart

[1] University of Maryland, College Park, MD USA riba@umd.edu
[2] Naval Surface Warfare Center, Carderock Div., West Bethesda, MD USA david.forrest@navy.mil azzam.mansour@navy.mil
[3] University of North Carolina Greensboro, Greensboro, NC USA arhall5@uncg.edu
[4] C3Nano, Hayward, CA USA melbs@3cnano.com
[5] Third Millenium Metals, LLC, Waverly, OH USA jshugart@tmmetals.com

ABSTRACT

Recent advances in nanomanufacturing have made it possible for large amounts (> 6 wt.%) of carbon to be incorporated as nanoscale carbon during a reaction process in molten aluminum, copper, silver, and other metals. These materials developed by Third Millennium Metals, LLC are called "covetics". The carbon is highly stable despite its form not being predicted in phase diagrams, and remains dispersed after remelting and resolidification. The carbon incorporates into the metal matrix and has an effect on several of the properties of the material. We have performed a detailed investigation of the structure and composition of several covetics using a variety of microscopy and spectroscopy techniques and found that the carbon forms nanoparticles of 5-200 nm diameter that are embedded in the host matrix. EELS spectra obtained from these regions show characteristic shape of carbon nanotubes (CNT). Raman data obtained from these samples also show the G-mode and D-mode characteristic of CNT.

Keywords: covetics, metal-carbon compounds, nanocarbon, Raman, EELS.

1 INTRODUCTION

Covetics are considered a new form of matter, comprised of high concentrations (>6 % wt) of carbon, integrated into metals in such a way that the carbon does not separate out during melting or magnetron sputtering. The resulting material has many unique and improved properties over the base metal from which it is produced. The carbon is dispersed through the metal matrix in several ways which together contribute to the enhanced properties. The carbon is bound into the material very strongly, resisting many standard methods at detecting and characterizing its form. The carbon is detectable by energy dispersive X-ray spectroscopy (EDS), electron energy los spectroscopy (EELS) and X-ray photoelectron spectroscopy (XPS), but not by analytic methods such as LECO and glow discharge mass spectrometry (GDMS)—due to its chemical affinity to the metal. The nanoscale carbon raises the melting points and surface tension. Covetics have higher warm-worked and cold-worked strengths. The microstructure is more resistant to softening and grain growth at elevated temperatures compared to the pure metal. The thermal conductivity is enhanced in the extrusion direction, and reduced in the transverse orientation in some covetics. The electrical conductivity is increased in aluminum, and maintained in copper.

2 EXPERIMENTAL

Cu 110, Ag (99.999%) and Al 6061 were converted to covetics containing carbon concentrations of: 2 wt. % and 5 wt. % for Cu covetic (denoted Cu 110 cv 2% and Cu cv 5%, respectively), 3 wt. % for Ag covetic (denoted Ag cv 3%) and 3 wt. % for Al 6061covetic (denoted Al 6061 cv 3%) by Third Millennium Metals, LLC using a proprietary procedure. We have performed XPS, X-ray absorption spectroscopy (XAS), scanning electron microscopy (SEM), transmission electron microscopy (TEM), scanning TEM (STEM), EELS, Helium Ion Microscopy and Raman scattering to investigate the structure and carbon incorporation in Al, Cu, and Ag covetics.

The XPS spectra were collected using a Physical Electronics Model 5400 spectrometer with Mg X-rays (1287 eV) from a 1.1 mm diameter spot and an electron takeoff angle of 45 degrees. The depth profiling was done with 4 keV Ar-ions using a rastered area of 5 mm x 5 mm. The sputtering rate was estimated to be ~ 2nm of SiO_2 per minute. The XAS experiments at the Cu K-edge and the Ag L3 edge were conducted on beamlines X11A and X19A, respectively, at the National synchrotron light source (NSLS).

Samples for TEM were prepared by mechanically polishing down to a thickness of ~ 30 μm followed by Ar ion milling (Ag and Cu covetics) or electro polishing (Al covetic) down to electron transparency. The TEM images were obtained using a JEOL 2100 LaB_6 TEM and a JEOL 2100 FEG TEM/STEM equipped with an Oxford energy dispersive X-ray detector (EDS) and a Gatan 863 Tridiem electron energy loss spectrometer.

3 RESULTS

Carbon was detected in the form of nanoparticles 5 nm - 200 nm in diameter with an interconnecting carbon matrix. There are two levels of incorporation of the nano-carbon in the metal matrix. Namelly, particles in the range of 50-200 nm are observed by SEM. We refer to these particles as particle nano-carbon (PNC). These particles, seen in Fig. 1, are fairly uniformly dispersed in the host metal and seem to have an amorphous structure. We have also observed regions of 5-100 nm containing carbon in which the carbon incorporates in the crystal lattice of the host material. We refer to these regions as "lattice structure nanocarbon" (LSNC). The nanoparticles are inter-connected through a carbon network (see Fig. 2); although the carbon interconnecting network is not always observed.

The incorporation of C in the LSNC regions is different for the different host material (Cu, Al and Ag) eventhough all three materials have fcc structures. Figure 3 shows an example of the LSNC in which a modulation of ~1.6 nm is observed along several directions in a Cu cv 5% sample. The diffraction pattern from the area, shown as inset to the figure, shows strong spots corresponding to the (110) zone axis of copper. The diffraction pattern also shows weak satellite spots corresponding to the modulation in the structure. The modulation is along the <111>, <002> and <220> directions of Cu. This region of the sample contained a relatively high concentration of C of ~7.44 wt % as measured by EDS in the TEM. Other regions of the sample did not show as high carbon content. The same type of LSNC was observed in many regions of a Cu cv 2% sample by HRTEM and high angle annular dark field (HAADF) STEM.

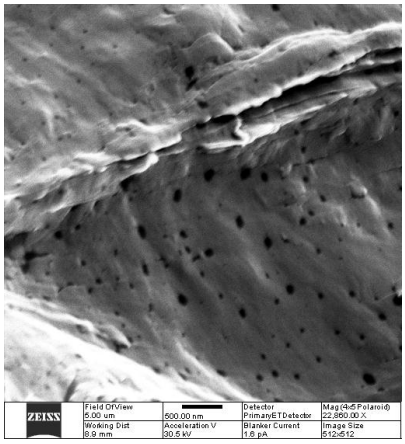

Fig. 1 He ion microscope image of the fractured surface of as-extruded Al 6061 covetic with ~3% C.

The LSNC, however, is different in Al and Ag covetics. In the case of Al cv 3% a stripe modulation is observed along preferred crystallographic directions as shown in the HAADF image in Fig. 4. The diffraction pattern from the area provided as inset to the figure shows the $(\bar{1}11)$ diffraction pattern of Al. It also shows weak spots corresponding to the $[10\bar{1}0]$ spots of graphite. These spots lie between the Al <220> spots. In addition to the weak spots a diffuse ring is observed in the diffraction pattern suggesting that amorphous carbon is also present in addition to crystalline graphite-like carbon. EELS spectra obtained from these regions indicated a lower concentration of carbon along the stripes.

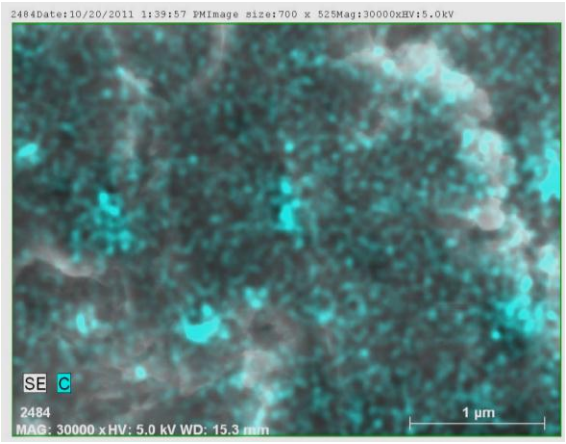

Fig. 2) SEM image of as-extruded Al 6061 cv ~3% with the C K_α map superimposed. The C-K map shows a network of interconecting C.

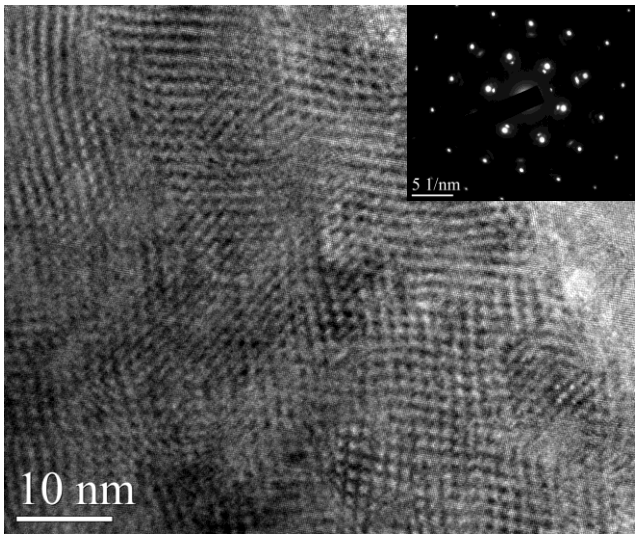

Fig. 3 (110) HRTEM image of a Cu cv 5% sample showing modulation of ~1.6 nm along several crystalline directions. The inset is the diffraction pattern from the area.

Ag covetic has yet a different incorporation of the carbon in the LSNC regions. Figure 5 shows a $[1\bar{1}0]$ high resolution TEM (HRTEM) image of Ag cv 3%. This region shows what seems to be alternating layers of graphene embedded in between the (111) planes of Ag. It is interesting to note that the (111) planes of Ag have low energy sites with a separation which is ~14% larger than the C-C interatomic distance in graphene.

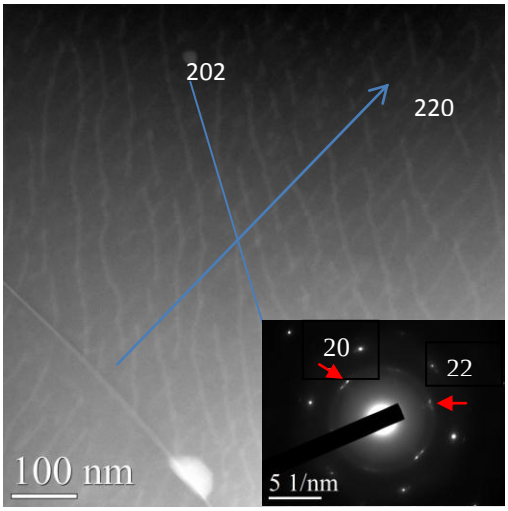

Fig. 4 HAADF STEM image from Al cv 3%. The inset is the diffraction pattern from the area and shows weak spots (arrowed) corresponding to "graphite" spots.

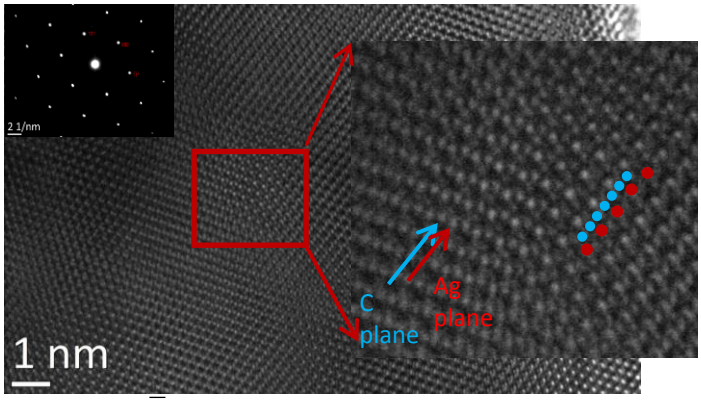

Fig. 5 $[1\bar{1}0]$ HRTEM image of Ag cv 3%. A region showing alternating planes between the Ag (111) planes is enlarged. This region seems to have graphene planes embedded in the Ag lattice. The inset is the diffraction pattern from the area.

In order to investigate how carbon is incorporated in the crystal structure of the host metal we obtained EELS data for the C-K edge in Al, Cu, and Ag covetics. The detailed strcture of the C-K edge is somewhat different for the three covetics. Figure 6 shows typical C-K edge spectra for Al, Cu and Ag covetics. The three spectra show similar characteristic shape consistng of a pre-peak at ~ 284 eV which has been identified as being due to the transition to π^* states from sp^2 bonded carbon [1] and suggest that graphite-like sheets are present in all three samples. The relative contribution to this pre-peak in the three spectra is different with a higher contribution in Ag followed by Al and then Cu. The spectra look very different from that of diamond [2]. However, they are similar to spectra from either graphite, amorphous carbon or even carbon nanotubes (CNT), i.e., materials that have sp^2 bonding.

In order to obtain more information on the type of bonding of the carbon in the covetics Raman spectra were obtained from several samples. Raman spectra from the as-extruded Al 6061 cv 3% sample are shown in Fig. 7. The spectra show a signal characteristic of the G-band at 1,600 cm^{-1} and a D-band at 1,300 cm^{-1}.[3,4] The G-band is characteristic of sp^2 bonding and is, therefore, observed in graphite and CNT. The D-band corresponds to a breading mode of A_{1g} symmetry which is forbidden in perfect graphite. The D-band is associated with defects and is frequently observed in CNT [5].

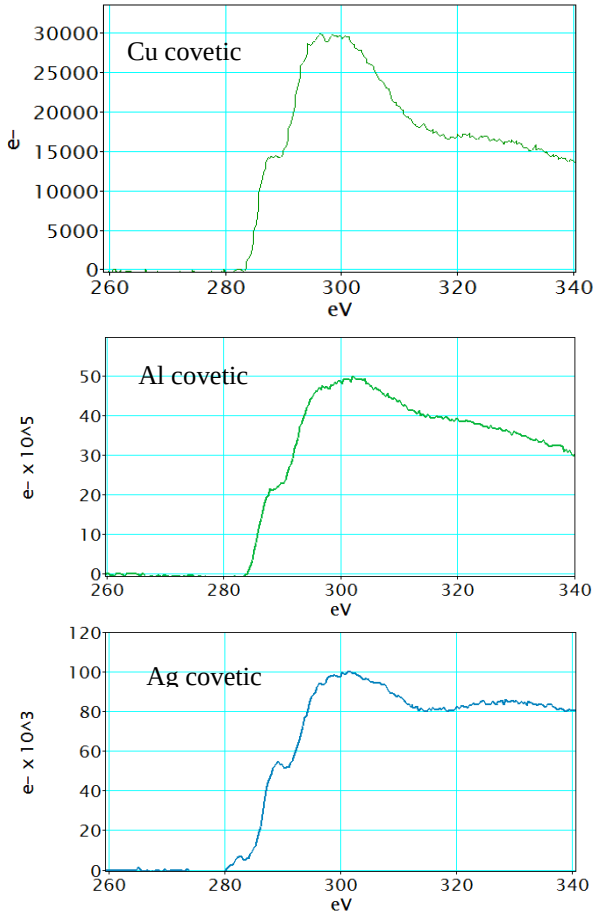

Fig. 6 EELS spectra at the C-K edge from Cu, Al and Ag covetics.

XPS depth profiling spectra were obtained from the Ag cv 3% sample to investigate the uniformity of the carbon distribution in the sample. Figure 8 shows that the C content is fairly uniform after the first minute of sputtering. The oxygen content is negligible except at the surface of the sample. Analysis of the XPS data shows that the actual concentration of C in the Ag covetic sample is ~ 8 ±1 at % (~0.96 ± 0.12 wt%). This result indicates that the actual incorporation of carbon in the Ag crystal structure was much lower than the nominal 3 wt. % value. The EXAFS spectra did not show any difference between the bond length of Ag-Ag in the covetic sample than in a standard Ag foil analyzed for comparison. This result does not agree with the HRTEM image from the Ag covetic sample in

Fig. 5. One possible reason is that XPS and EXAFS analyze a relatively large area of the sample (the spot was 1.1 mm in diameter) while the domains with graphene layers between the Ag (111) layers was observed in small regions of the sample of ~ 20-40 nm.

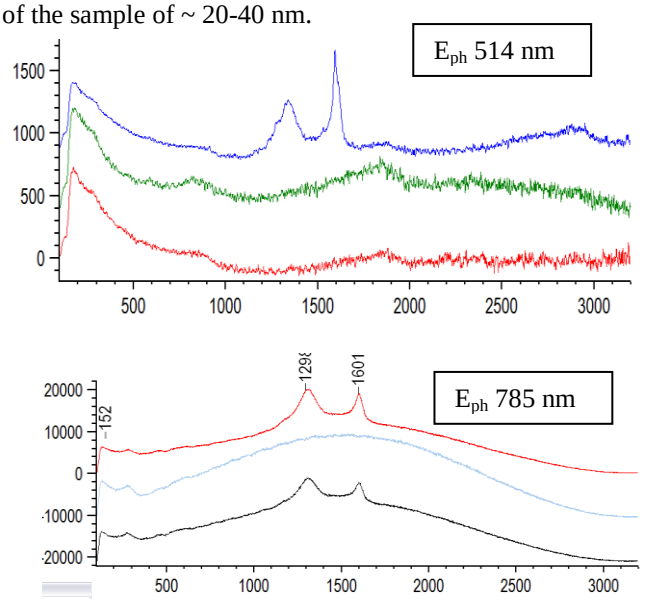

Fig. 7 Raman spectra from the as-extruded Al cv 3% obtained at three different locations and for two different laser wavelengths. The Raman shift is in cm^{-1}.

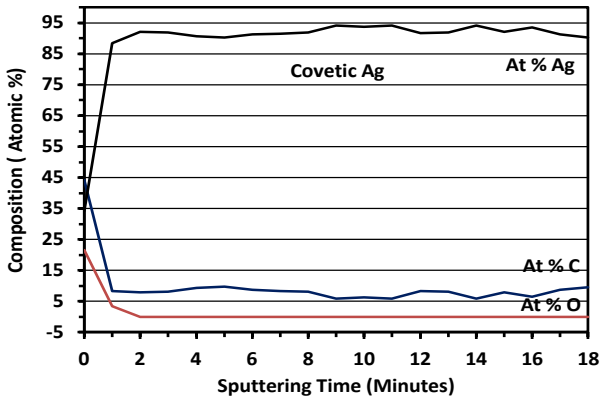

Fig. 8 Composition depth profile obtained from XPS depth profiling from a Ag cv 3% sample.

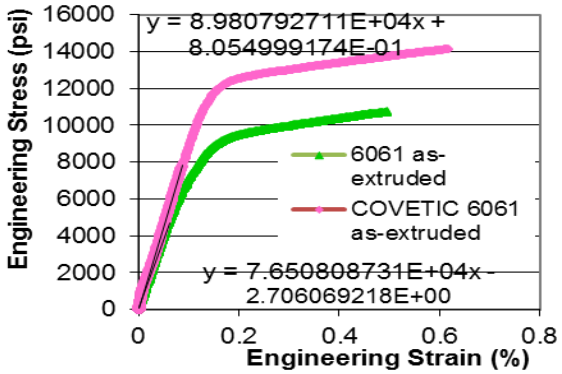

Fig. 9 Engineering stress for as-extruded Al 6061 and Al 6061 cv 3%.

The incorporation of C into metals by conversion to covetics enhances the strength of the material as shown in Fig. 9 for as-extruded Al 6061 cv 3% compared to regular as-extruded Al 6061. The Al 6061 covetic showed 30% higher yield strength than regular Al 6061. Similar results were obtained for Al 7075 covetic and Cu covetic.

SUMMARY AND CONCLUSIONS

The incorporation of carbon in covetics takes different forms depending on the host metal. In Cu covetic carbon gives rise to modulation along several crystallographic directions in the Cu lattice. In Al covetic carbon gives rise to stripes which tend to be oriented along preferred crystallographic directions in the Al lattice. In Ag covetic graphene-like layers intercalate between the Ag (111) planes. Even with these different forms of carbon incorporation, the C K-edge in the EELS data from Cu, Al and Ag covetics show a characteristic pre-peak of the sp^2 to π^* transition similar to the edges observed in graphite, amorphous carbon and CNT although the detailes in the C K-edge of the three materials investigated show some differences. Raman scattering from Al covetic shows signals indicative of CNT. XPS depth profile shows a uniform distribution of carbon in Ag covetic although at a much lower concentration than expected.

ACKNOWLEDGMENTS

This work was supported in part by NSF MRSEC DMR 0520471 and ONR Code 332 # N0001410WX20992. We acnowledge support from the University of Maryland Nanocenter and the NISP Lab. ANM acknowledges support by the Carderock Division of the Naval Surface Warfare Center's In-house Laboratory Independent Research Program administrated under ONR's Program Element 0601152N. The XAS experiments were conducted at the NSLS, which is supported by the U.S. Department of Energy, Office of Basic Energy Sciences, under contract no. DE-AC02-98CH10886. We gratefully acknowledge the assistance of Dr. Andrew A. Herzing (NIST, Gaithersburg, MD) in performing atomic-resolution STEM-HAADF imaging.

REFERENCES

[1] D.A. Muller, Y. Tzou, R. Raj, and J. Silcox, Nature 366, **725** (1993).

[2] R.R. Schlittler, J.W. Seo, J.K. Gimzewiski, C. Durkan, M.S.M. Saifullah, M.E. Welland, Science **292**, 1136 (2001).

[3] A.C. Ferrari, and J. Robertson, Phys. Rev. B **61**, 14095 (2000).

[4] J. Wagner, M. Ramsteiner, Ch. Wild, and P. Koidl, Phys. Rev. B **40**, 1817 (1989).

[5] M.S. Dresselhaus, G. Dresselhaus, R. Saito and A. Jorio, Phys. Reports, Rev. Sec. Phys. Lett. **409**, 47 (2005).